Agricultural and Forest Meteorology 373 (2025) 110758

Contents lists available at ScienceDirect

Agricultural and Forest Meteorology

journal homepage: www.elsevier.com/locate/agrformet

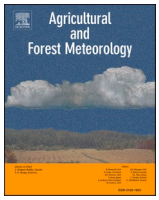

A managed boreal forest landscape in northern Sweden is a persistent net carbon sink despite large inter-annual weather anomalies

Jinshu Chi [a,b,*], Anne Klosterhalfen [a,c], Mats B. Nilsson [a], Hjalmar Laudon [a], Jörgen Wallerman [d], Johannes Larson [a], Anders Lindroth [e], Natascha Kljun [f], Johan E.S. Fransson [d,g], Tomas Lundmark [a], Matthias Peichl [a]

[a] Department of Forest Ecology and Management, Swedish University of Agricultural Sciences, Umeå, Sweden
[b] Earth, Ocean and Atmospheric Sciences Thrust, The Hong Kong University of Science and Technology (Guangzhou), Guangzhou, China
[c] Bioclimatology, University of Göttingen, Göttingen, Germany
[d] Department of Forest Resource Management, Swedish University of Agricultural Sciences, Umeå, Sweden
[e] Department of Physical Geography and Ecosystem Science, Lund University, Lund, Sweden
[f] Centre for Environmental and Climate Science, Lund University, Lund, Sweden
[g] Department of Forestry and Wood Technology, Linnaeus University, Växjö, Sweden

ARTICLE INFO

Keywords:
Boreal forest landscape
Terrestrial and aquatic carbon fluxes
Harvest carbon export
Tall-tower eddy covariance
Catchment stream monitoring
Inter-annual weather variations

ABSTRACT

The future role of boreal forests in the global carbon cycle is uncertain given the rapid climate change in high latitudes. At the landscape scale, heterogeneity in stand age and land cover, contributions from terrestrial and aquatic fluxes, and harvest export may create complex carbon cycle-climate interactions. However, the integrated response of the net landscape carbon balance (NLCB) to inter-annual variations (IAVs) in environmental conditions is poorly understood. Here, we used tall-tower eddy covariance and stream monitoring to integrate terrestrial and aquatic carbon fluxes with harvest export for a 68 km^2 boreal catchment in Sweden during 2016–2020. This actively managed forest landscape acted as a net carbon sink with a 5-year mean (± standard deviation) NLCB of 128±55 g C m^{-2} yr^{-1}. The NLCB IAV included a reduced sink (36 g C m^{-2} yr^{-1}) during the cool/cloudy year 2017. In the other four years, featuring a drought summer (2018) and an exceptionally warm/wet winter (2020), the landscape acted as a significant sink (127–180 g C m^{-2} yr^{-1}). The NLCB IAV corresponded primarily to variations in landscape respiration, followed by GPP and harvest export, with negligible contributions from landscape CH_4 and aquatic carbon fluxes. The NLCB IAV was not correlated to any single environmental factor. However, daily NLCB contrastingly responded to key environmental factors as a function of forest aboveground biomass and mire contributions. Overall, our study indicates that the annual carbon sink-strength of the managed boreal forest landscape may be resilient to a wide range of IAVs in environmental conditions.

1. Introduction

Climate change in the boreal region has been projected to occur at a faster rate than in other regions of the globe (IPCC, 2023). Boreal forest landscapes have great potential to mitigate climate change through their high carbon sequestration capacity (Gauthier et al., 2015). Meanwhile, boreal landscapes actively exchange two important greenhouse gases (GHGs), i.e., carbon dioxide (CO_2) and methane (CH_4), with the atmosphere (Helbig et al., 2017; Pan et al., 2011). Because these landscapes typically consist of both forest and mire ecosystems, understanding their combined capacity and controls of CO_2 sequestration as well as CH_4 uptake and emissions is essential for evaluating their role in regulating atmospheric GHG concentrations and associated climate change (Zhao et al., 2023).

Detailed knowledge of the magnitudes and controls of the carbon balance at the landscape scale (i.e., tens of km^2) requires comprehensive carbon flux estimates spanning the large heterogeneity in ecosystem properties and functioning (Chapin et al., 2006; Christensen et al., 2007; Drysdale et al., 2022; Webb et al., 2019, 2018). Most commonly, such estimates rely on bottom-up estimates based on plot- or ecosystem-level measurements (Christensen et al., 2007; Heiskanen et al., 2023). However, such approaches are cumbersome and their numerous estimates of

* Corresponding author.
E-mail address: jinshuchi@hkust-gz.edu.cn (J. Chi).

https://doi.org/10.1016/j.agrformet.2025.110758
Received 17 November 2024; Received in revised form 18 July 2025; Accepted 23 July 2025
Available online 1 August 2025

underlying component fluxes aggregate considerable uncertainty (Goulden et al., 1996), which hinders a complete understanding of the boreal landscape carbon cycle-climate feedback. To overcome these challenges, Chi et al. (2020) introduced a method that combines tall-tower eddy covariance measurements with stream monitoring to derive a direct estimate of the net landscape carbon balance (NLCB) by integrating the terrestrial and aquatic fluxes of CO_2, CH_4, dissolved organic carbon (DOC), dissolved inorganic carbon (DIC), and carbon export via harvest across all ecosystems within a heterogeneous landscape. The NLCB concept has been subsequently adopted in a tropical savanna in Australia (Duvert et al., 2020) and a highly erodible semiarid catchment in China (Ran et al., 2022). The need for integrating terrestrial and aquatic carbon fluxes has been further highlighted in other recent studies (Balathandayuthabani et al., 2023; Casas-Ruiz et al., 2023; Gao et al., 2022; Heiskanen et al., 2023; Liu et al., 2023; Lv et al., 2023; Song et al., 2021; Tong et al., 2024).

However, to date, NLCB estimates have been limited to short-term (<3 years) study periods, which limits our understanding of how the carbon sink-source strength responds to various environmental conditions, especially to extreme events that may occur at infrequent intervals. For example, a large between-year variation in NLCB (4 vs. 73 g C m^{-2} yr^{-1}) observed in a Swedish boreal landscape due to the abiotic controls of air temperature and global radiation (Chi et al., 2020) indicates the potential for considerable sensitivity of the landscape-scale carbon balance to changing environmental conditions in the boreal region. Moreover, extreme weather conditions such as the drought summer or the warm and wet winter occurring throughout Europe during 2018 and 2020, respectively, have significantly impacted the boreal ecosystems within the landscape (e.g., Gharun et al., 2025; Lindroth et al., 2020; Martínez-García et al., 2022; Rinne et al., 2020). For example, the 2018 summer drought has resulted in the age-dependent reduction of forest carbon sink strength across the boreal landscape (Martínez-García et al., 2024), turned a nearby mire from a 15-year persistent annual net carbon sink to a net carbon source (Rinne et al., 2020), and altered the biogeochemistry of the boreal stream network towards anaerobic metabolism (Gómez-Gener et al., 2020). The warm and wet winter of 2020 has caused increased ecosystem respiration but little impact on photosynthesis in mature boreal forest stands (Gharun et al., 2025). More recently, the increasing atmospheric dryness has caused reduced boreal forest tree growth both in Sweden and Canada (Laudon et al., 2024; Mirabel et al., 2023). Given the various responses of different forest stands and other ecosystem types to the environmental conditions, the overall effects of these changing environmental conditions on the landscape-scale carbon balance remain poorly understood and long-term monitoring of the NLCB is essential to obtain a better understanding of its resilience to changes in weather and climatic extreme events.

In this study, we compiled a 5-year (2016–2020) dataset of continuous measurements of terrestrial and aquatic fluxes of CO_2, CH_4, dissolved organic and inorganic carbon, and carbon export via tree harvest based on tall-tower eddy covariance measurements, a stream monitoring network, and satellite imagery and LiDAR data products for a managed forest landscape in northern Sweden. The main objectives were to 1) quantify the inter-annual variations of the carbon sink-source strength of a managed boreal forest landscape, 2) determine the environmental factors regulating the inter-annual variations of NLCB, and 3) investigate how landscape heterogeneity regulates the response of the NLCB to various environmental patterns.

2. Materials and methods

2.1. Site description

The study was conducted at the Integrated Carbon Observation System (ICOS) Svartberget station (https://www.icos-sweden.se/svartberget) located in the Krycklan catchment (Fig. S1), a well-established research infrastructure representing a typical boreal forest landscape (68 km^2) in northern Sweden (Laudon et al., 2021a). The site has a boreal climate with a 30-year (1991–2020) mean annual air temperature of 2.4 °C and mean annual precipitation of 638 mm recorded from the nearby Hygget automatic climate station. Land cover types include forest stands (87 %) with different species (63 % Scots pine *Pinus sylvestris*, 26 % Norway spruce *Picea abies*, and 10 % Birch *Betula* spp.) and age classes (5–211 years), clear-cuts (1 %), mires (9 %), lakes (1 %), streams, and arable lands (2 %) (Laudon et al., 2021a). Around 85 % of forest stands within the catchment have been actively managed, including the practices of clear-cutting, thinning, and small areas of fertilization and ditch network maintenance (Laudon et al., 2021a). More information about the site conditions and research infrastructures in the Krycklan catchment is described in Chi et al. (2019) and Laudon et al. (2021a). The annual period is defined as the calendar year, which is further separated into growing season (GS) and non-growing season (NGS). The GS was defined as the period from the beginning of April to the end of October, during which the majority of the gross primary production occurs, with the remainder of the annual period defined as the NGS.

2.2. Landscape-scale carbon flux measurements

2.2.1. Eddy covariance and ancillary measurements

On the 150 m tall ICOS-Svartberget monitoring tower, one eddy covariance (EC) system (CPEC 200, Campbell Scientific, Inc., hereafter, CPEC system) measuring the landscape-scale net CO_2 fluxes was installed at 70 m above the ground in March 2016 and lowered to 60 m in October 2017. The CPEC system was instrumented with an ultrasonic anemometer (CSAT3, Campbell Scientific, Inc.) and a closed-path infrared gas analyzer (EC155, Campbell Scientific, Inc.). In August 2017, a second EC system (hereafter, LGR system) consisting of a sonic anemometer (uSonic-3 Omni, METEK GmbH) and a gas analyzer (FGGA-24EP, Los Gatos Research, Inc.) was mounted at the height of 85 m to measure the net CO_2 and CH_4 exchanges between the landscape and the atmosphere. Both CPEC and LGR systems sampled the raw data at a rate of 10 Hz.

The landscape-scale net CO_2 and CH_4 flux data measured from the two EC systems were processed following the procedures developed by Chi et al. (2019) and Chi et al. (2020). Briefly, we used the EddyPro® software (v7.0.6, LI-COR Biosciences) to process the 10 Hz raw data into the half-hourly net CO_2 and CH_4 fluxes, which were further corrected for their storage terms in the air volume underneath the EC measurement heights. Half-hourly CO_2 and CH_4 storage terms were estimated based on Montagnani et al. (2018) using the CO_2 (at 10, 15, 20, 25, 30, 35, 42, 50, 60, (70), (85) m) and CH_4 (at 35, 85 m) concentration profile measurements. The storage-corrected net CO_2 and CH_4 fluxes were quality-controlled for the following criteria: non-steady state and undeveloped turbulent conditions (Mauder and Foken, 2004), low uptime of sonics and gas analyzers, wind distortion, site disturbances, predominant horizontal and vertical advections (Wharton et al., 2009), and statistical outliers outside the range of mean $\pm$ 3 $\times$ standard deviations over a moving window of 10 days (Chi et al., 2019). In addition, the uncertainty related to vertical flux divergence across the three EC measurement heights was assessed using the method described in Drysdale et al. (2002). Compared to our approach, flux divergence correction resulted in small biases for the three EC measurement heights with the median bias in half-hourly CO_2 fluxes ranging from −4.7 % to 2.8 % (Fig. S2). A comprehensive comparison between the two EC levels at 60 and 85 m has been conducted in Klosterhalfen et al. (2023), and the regression and diurnal plots comparing data from the different heights during overlapping periods were illustrated in Fig. S3.

Starting in August 2017, gaps in the CO_2 fluxes measured from the CPEC system were primarily filled with the fluxes measured from the LGR system. The potential positive bias in annual CO_2 flux sums due to this data combination was estimated to be 5–11 % of annual NEE in

2017–2019. The uncertainty in annual NEE resulting from this approach was thus within the range of commonly observed from other standard gap-filling techniques based on environmental drivers (Moffat et al., 2007). Despite the bias, this gap-filling procedure was preferred since it allowed us to preserve the footprint information and relate these to the fluxes during these periods. Prior to August 2017 and during subsequent periods without LGR data available, the gaps in the CO_2 and CH_4 fluxes were filled using the marginal distribution sampling (MDS) approach with two sets of look-up factors: 1) global radiation, air temperature, and vapor pressure deficit for gap-filling the net CO_2 fluxes (Reichstein et al., 2005), 2) air temperature, vapor pressure deficit, and source area contribution of mires estimated using the FFP model (see Section 2.4) for gap-filling the net CH_4 fluxes (Chi et al., 2020). The gap-filled net CO_2 fluxes were partitioned into landscape respiration (RE) and gross primary production (GPP) using the nighttime-based partitioning approach (Reichstein et al., 2005) in REddyProc (Wutzler et al., 2018) due to the better agreement between the modeled and measured nighttime CO_2 flux data compared to the daytime-based method (Chi et al., 2019).

The annual sums of net CO_2 and CH_4 fluxes, GPP, and RE were corrected for the tower location bias inherent to the tall-tower EC measurements resulting from the land cover heterogeneity as described in detail by Chi et al. (2019). Briefly, the tower location bias correction was performed using the footprint model (see Section 2.4) and the ecosystem-level EC flux data measured at the nearby forest (ICOS-Svartberget) and mire (ICOS-Degerö) sites during 2016–2020. The ICOS-Svartberget EC system is mounted 34.5 m above the ground on the same tall tower as the landscape-scale EC measurements. The ICOS EC systems deployed at the Svartberget and Degerö sites are both instrumented with a sonic anemometer (Gill WindMaster Pro, Gill Instruments Ltd., Germany) and a LI-COR closed-path IRGA (LI-7200 Closed-Path CO_2/H_2O Gas Analyzer, LI-COR Biosciences, USA). Flux data collected by the ICOS-Svartberget and ICOS-Degerö systems were processed following the procedures described in Chi et al. (2019) and Rinne et al. (2020), respectively. The tower location bias was corrected for the annual scale data instead of half-hourly fluxes to avoid extended gaps which are often too long to be reasonably filled using the commonly applied methods, such as the MDS method. The correction factors for the landscape-scale fluxes were shown in Table S1. The uncertainties related to vertical flux divergence (15 % increase in annual NEE) have been evaluated and compared with our storage and advection correction approach (Fig. S4). However, the uncertainties due to advection filtering (~19 % reduction in annual NEE, Chi et al., 2019), random measurement errors and gap-filling procedures (~ ± 6 % of annual NEE, Chi et al., 2019), as well as the bias in the two-level EC measurements (~100 % of annual NEE in the absence of tower location bias correction, Klosterhalfen et al., 2023) have been explicitly assessed in previous studies, and thus these analyses were not repeated in this study.

Following Chapin et al. (2006), the landscape-scale GPP, RE, and net CO_2 and CH_4 fluxes obtained from the eddy covariance measurements follow the micrometeorological sign convention that positive and negative values represent carbon release from and uptake by the landscape, respectively, whereas the opposite ecological sign convention applies to NLCB. We further defined the environmental NLCB ($NLCB_e$) as the NLCB excluding harvest carbon export for sub-annual analysis, as harvest carbon export was available for annual scale only. As CH_4 flux measurements were only conducted during 2018 and 2019, we applied the two-year mean annual CH_4 flux from those years in the estimates of the $NLCB_e$ and NLCB for the other three years.

Meteorological data were continuously recorded at 30-min intervals during 2016–2020, including photosynthetic photon flux density (PPFD) measured at 50 m above the ground, precipitation (PPT), air temperature (T_{air}) and relative humidity (RH) at the height of 70 m (or 60 m after August 2017). Global radiation (R_g) was calculated from the PPFD measurements by multiplying a factor of 0.52. Vapor pressure deficit (VPD) was derived from the half-hourly averaged T_{air} and RH measurements. Soil temperature (T_{soil}) and soil water content (SWC) were retrieved from the ERA5 hourly data (the fifth generation ECMWF reanalysis for the global climate and weather, https://cds.climate.copernicus.eu/cdsapp#!/dataset/reanalysis-era5-single-levels). Hourly data were resampled to half-hourly data by linear interpolation. T_{soil} and SWC in soil layer of 0–7 cm at the corresponding grid cell (64.25° N, 19.75° E) with a grid cell size of 0.25° by 0.25° representing the landscape-scale soil conditions were used in this study (Fig. S5). Comparisons between the ERA5 and the ICOS point-level T_{soil} and SWC data were illustrated in Fig. S6. Long-term (1991–2020) T_{air} and PPT data were obtained from the nearby Hygget automatic weather station. Long-term T_{soil}, SWC, R_g, and VPD data were retrieved from the ERA5 data (Bell et al., 2021). In this study, we defined the warm or cool and dry or wet conditions when the seasonal or annual T_{air} and PPT anomalies were beyond the interquartile ranges of environmental conditions over the 30-year period from 1991 to 2020. Extreme environmental conditions were identified as seasons or years with the weather data exceeding the 30-year records (Table S2).

2.2.2. Aquatic carbon flux measurements

During the study period, stream discharge rate was monitored at hourly intervals and averaged into daily estimates at the catchment outlet (Fig. S1). Rainfall and/or snowfall were sampled for each precipitation event and bulked into monthly samples, while stream water was sampled weekly during spring, biweekly during summer and autumn, and monthly during winter (Laudon et al., 2021b). DOC, DIC, and dissolved CO_2 and CH_4 concentrations in these water samples were analyzed to calculate the DOC wet deposition rate and the aquatic carbon exports, including DOC, DIC, and dissolved greenhouse gases (i.e., CO_2 and CH_4) through stream discharge. The particulate organic carbon in the streams is small in the boreal Scandinavia region (Wallin et al., 2013), which accounts for < 0.6 % of total organic carbon (TOC) across the Krycklan catchment (Laudon et al., 2011) and thus was not included in this study. More details on aquatic carbon flux calculations are documented in Wallin et al. (2010, 2013).

2.2.3. Carbon export via clear-cutting

The annual carbon export via tree harvest was estimated based on the area that was clear-cut each year during the 5-year study period multiplied by harvest volume. Annual clear-cut areas were retrieved from the Swedish Forest Agency (https://www.skogsstyrelsen.se/sjalvservice/karttjanster/skogliga-grunddata), based on change detection analysis using satellite imagery. The annual clear-cut area within the Krycklan catchment was summed for each year. A constant harvested wood volume per hectare (184 m^3 ha^{-1}) previously determined for the years 2016–2018, a wood density of 0.4 t m^{-3} and a wood carbon concentration of 47 % were assumed for any clear-cut area across the study landscape during the study period (Chi et al., 2020). More information about estimating the amount of carbon export via clear-cutting is explicitly described in Chi et al. (2020). It is noteworthy that the harvest carbon export via thinning and other harvest-related disturbances (e.g., windfall) was not included in this study, as the records of such operations and associated harvested volumes were not available for the study period. According to the national forest inventory, thinning and other harvest contributed ~20 % and 10 % of the annual harvest volume in Sweden (Nilsson et al., 2025).

2.3. Land cover and forest aboveground biomass

Land cover types for the study area were retrieved from the Geografiska™ Sverigedata (GSD) data products. A raster layer showing six land cover types (i.e., forests, mires, lakes, cultivated areas, clear-cuts, and residential areas) was resampled from vector data to a raster layer with a pixel size of 10 m by 10 m (Fig. S1a). Forest aboveground biomass (AGB) was estimated for the year 2019 using the area-based method where the high-resolution light detection and ranging (LiDAR) data (~20 points/m^2) were related to measurements from > 400 field-

inventoried sample plots (radius = 10 m) allocated across the entire Krycklan catchment (Fig. S1b). The pixel size of forest AGB raster data was set to 12.5 m by 12.5 m (Martínez-García et al., 2022).

2.4. Flux footprint analysis

The two-dimensional parameterization for Flux Footprint Prediction (FFP, Kljun et al., 2015) was applied to estimate the source area contribution from each grid cell within the Krycklan catchment. Improved from the previous study (Chi et al., 2019) where the boundary layer height (h_{bl}) input was kept as a constant parameter for daytime and nighttime, respectively, the hourly h_{bl} data from the ERA5 data were retrieved from the same grid as the T_{soil} and SWC dataset to include the diurnal variations of h_{bl} in the footprint estimates. The hourly h_{bl} data were resampled to half-hourly data through linear interpolation to match the temporal scale of other model input parameters, such as friction velocity, wind direction, and the Monin-Obukhov length (Klosterhalfen et al., 2023). More information on the tall-tower flux footprint estimation is given in Chi et al. (2019, 2020). The source area contribution of each land cover type to the flux measurements, e.g., from mires (f_{mire}), is the sum of grid cells containing the selected land cover (e.g., mire) weighted by its footprint function value (Chasmer et al., 2011; Chi et al., 2019). The forest AGB contribution ($f_{biomass}$) is the sum of the forest AGB estimates across all grid cells within the 90 % footprint contour line weighted by their corresponding source area contributions. Both land cover and forest AGB contributions were calculated on a half-hourly scale.

3. Results

3.1. Intra- and inter-annual variations in environmental conditions

Compared to the 30-year long-term records (1991–2020), the five study years (2016–2020) encompassed large intra- and inter-annual weather anomalies (Fig. 1). Specifically, annual T_{air} and PPT differed from their long-term means ranging from −0.12 to 1.70 °C and from −75 to +176 mm, respectively. The mean GS T_{air} (9.8 °C), R_g (170 W m^{-2}), and VPD (5.2 hPa) in 2018 and the mean NGS T_{air} (−2.5 °C) and PPT

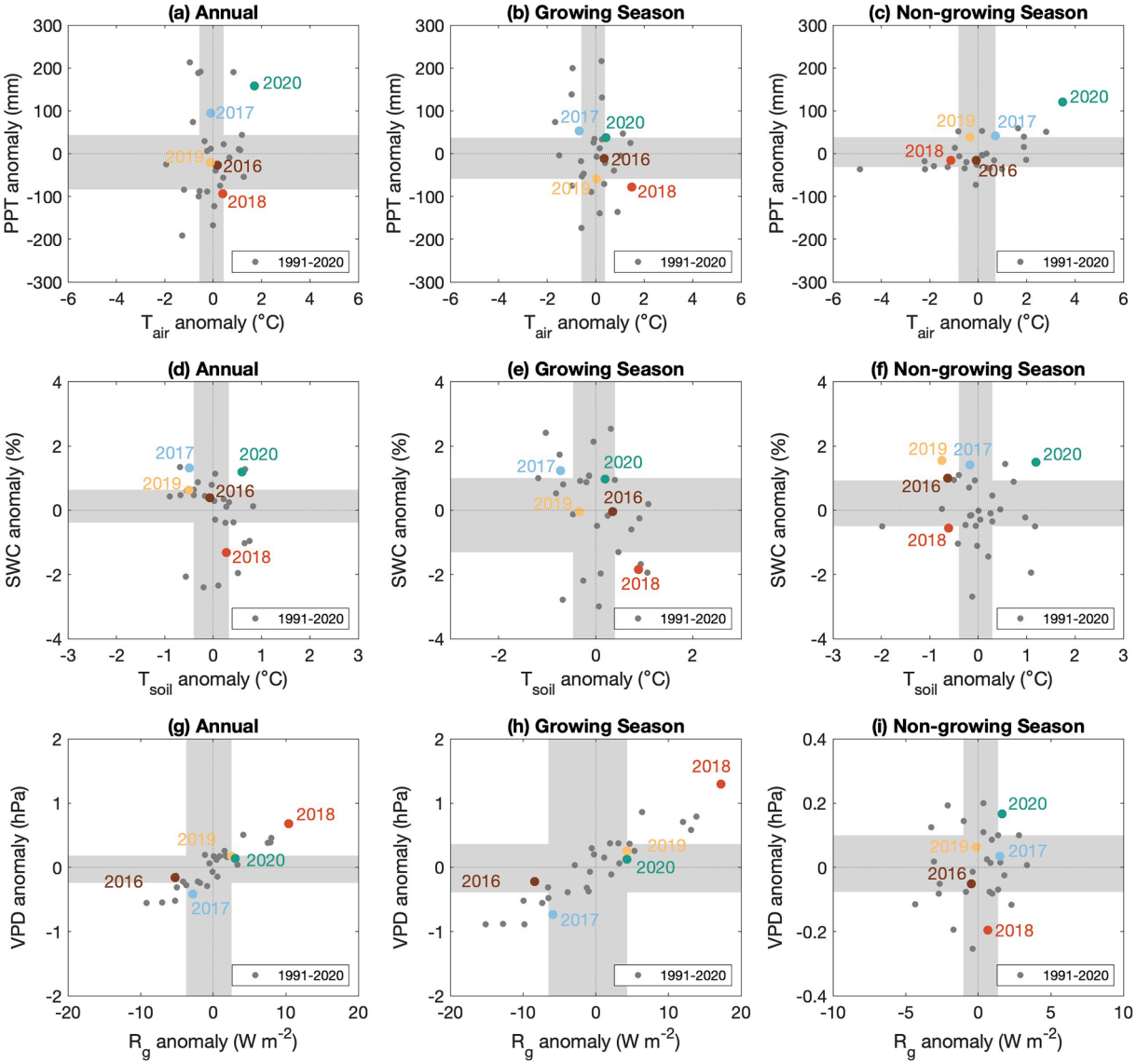

Fig. 1. Environmental anomalies of air temperature (T_{air}), precipitation (PPT), soil temperature (T_{soil}), soil water content (SWC), global radiation (R_g), and vapor pressure deficit (VPD), during the annual period (Jan-Dec), growing season (Apr-Oct), and non-growing season (Jan-Mar, Nov-Dec) from 2016 to 2020 at the study site. Anomalies are relative to the 30-year (1991–2020) averages recorded from the nearby Hygget automatic climate station or the ERA5 data. Grey areas represent the interquartile ranges of environmental conditions over 30 years.

(342 mm) in 2020 exceeded the 30-year historical records and thus were identified as seasons with extreme environmental conditions (Fig. 1, Table S2). Furthermore, both air and soil conditions were cool and wet during the GS of 2017 (outside the interquartile ranges of the long-term records), which contrasts with the normal or warm GS conditions during the other four years (Fig. 1, Table S2).

3.2. Seasonal and inter-annual variations in NLCB and its components

Averaged over the five-year study period, April and September were the transition months from which the landscape switched to a net carbon sink (positive $NLCB_e$) and a net carbon source (negative $NLCB_e$), respectively (Fig. 2a). The largest $NLCB_e$ was observed in June during the middle of summer (92 ± 10 g C m^{-2} $month^{-1}$), whereas the highest net carbon source was recorded in winter December (-23 ± 10 g C m^{-2}

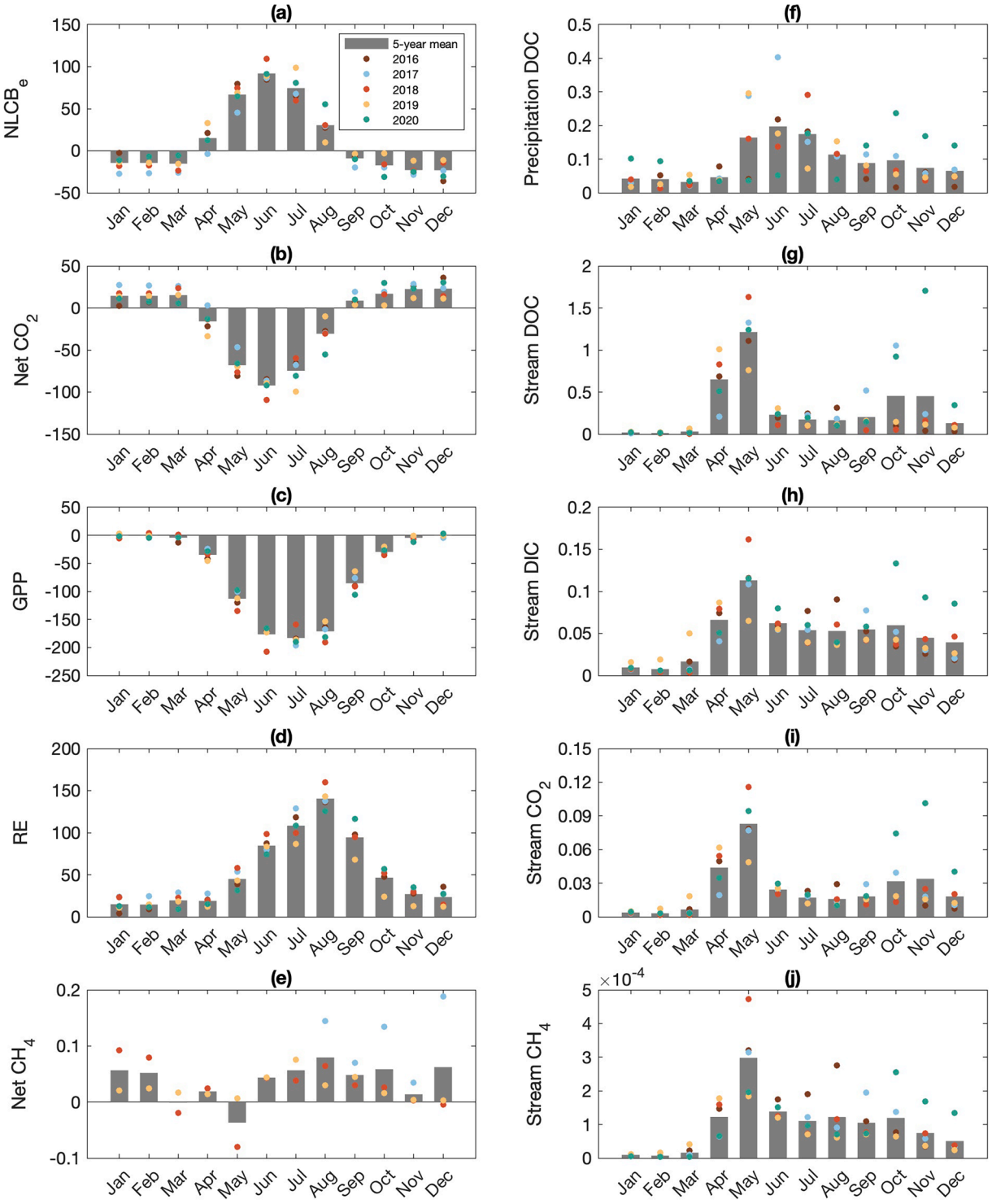

Fig. 2. Monthly sums of the environmental net landscape carbon balance ($NLCB_e$) (a) and its underlying terrestrial (b-e) and aquatic (f-j) carbon fluxes during 2016–2020. Grey bars represent the 5-year averages of the monthly carbon fluxes. Positive $NLCB_e$ indicates net carbon accumulation into the landscape (ecological sign convention). Positive vertical flux indicates net carbon release from the landscape (micrometeorological sign convention). All units are in g C m^{-2} $month^{-1}$.

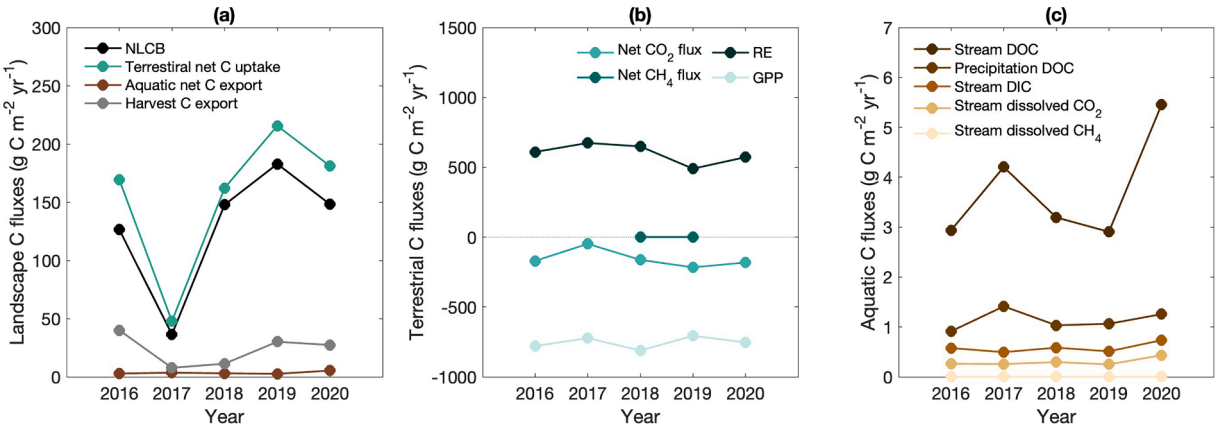

Fig. 3. Inter-annual variations in the annual net landscape carbon balance (NLCB), net terrestrial and aquatic carbon fluxes, and harvest carbon export (a), its separate terrestrial (b) and aquatic (c) flux components during 2016–2020. Positive NLCB values indicate net carbon accumulation into the landscape (ecological sign convention). Positive vertical fluxes indicate net carbon release from the landscape (micrometeorological sign convention).

month^{-1}). The seasonal pattern in $NLCB_e$ was largely driven by the landscape-atmosphere net CO_2 flux (Fig. 2b). However, the seasonal peaks of GPP (-183 ± 14 g C m^{-2} month^{-1}) and RE (141 ± 14 g C m^{-2} month^{-1}) showed a one- and two-month lag to seasonal peak of net CO_2 flux (-92 ± 10 g C m^{-2} month^{-1}), respectively (Fig. 2b-d). The monthly landscape-atmosphere net CH_4 emissions peaked in August (0.08 ± 0.06 g C m^{-2} month^{-1}) with occasional net CH_4 uptake during spring (Fig. 2e).

The distinct seasonal pattern of aquatic carbon fluxes from terrestrial carbon fluxes illustrated an initial low aquatic carbon exports from January to March (0.04 ± 0.03 g C m^{-2} month^{-1}), followed by a sharp increase during snow melt in April and May (up to 1.91 g C m^{-2} month^{-1}), a large (92 %) reduction during low flows in summer (down to 0.15 g C m^{-2} month^{-1}), and an occasional second seasonal peak during the wet autumn and winter, which for some years can be as high as the spring peak (Fig. 2f-j). Due to the relatively small magnitude of the aquatic carbon fluxes, this particular temporal variability explained however < 12 % of the variance in the seasonal variation of $NLCB_e$.

The 5-year mean annual NLCB was 128 g C m^{-2} with a large IAV ranging from 36 to 180 g C m^{-2}. The lowest net carbon sink strength was recorded during the wet year 2017, whereas the landscape acted as a persistently larger net carbon sink during the other four years (Fig. 3a, Table 1). Similar to its seasonal variation, the NLCB IAV was also dominantly driven by the variations in terrestrial net carbon exchange with the atmosphere (Pearson's correlation coefficient, $r = 0.98$, $p = 0.03$), followed by variations in carbon export via harvest ($r = 0.54$, $p = 0.35$) (Fig. 3a). Furthermore, the IAV of terrestrial net carbon exchange was more strongly correlated to RE ($r = 0.80$, $p = 0.10$) than GPP variations ($r = 0.11$, $p = 0.85$) (Fig. 3b). The lowest and highest annual NLCB occurring in 2017 and 2019 corresponded with the enhanced RE from January to July 2017 and the reduced RE from July to December 2019, respectively (Fig. 2d, Table 1). The IAV of the aquatic carbon export was, similar to that of the NLCB, primarily determined by variations in the annual DOC export, with the latter being driven by the variations in stream discharge while DOC concentrations remained relatively constant (Fig. 3c).

3.3. *Response of the NLCB to key environmental factors*

Global radiation (R_g) was a significant driving factor that enhanced daily $NLCB_e$ from April to November for the entire GS and post-GS (Fig. 4). In contrast to the R_g response, precipitation (PPT) showed a negative correlation with daily $NLCB_e$ throughout most of the GS months (May-October). Air temperature (T_{air}) was negatively correlated with daily $NLCB_e$ during GS and this constraint was especially pronounced during the NGS. However, T_{air} showed the highest positive cross-correlation coefficient with daily $NLCB_e$ with a one-month lag (Fig. S7). The influence of soil temperature (T_{soil}) on daily $NLCB_e$ was important only during pre- and early-GS (March-May). At the annual scale, NLCB showed a positive relationship with T_{air}, T_{soil}, R_g, and VPD, but was negatively correlated with PPT and SWC (Fig. S8).

Season-specific environmental conditions contributed to the IAVs of NLCB and its carbon flux components. In general, the warm weather

Table 1
Annual budgets of landscape-scale terrestrial and aquatic carbon fluxes from 2016 to 2020.

Flux*	2016	2017	2018	2019	2020	5-year mean ± std.
Vertical fluxes						
Landscape-atmosphere net CO_2 exchange	−170	−48	−161	−213	−182	−155 ± 63
Landscape GPP	−780	−720	−803	−694	−754	−750 ± 44
Landscape RE	610	672	642	481	572	595 ± 74
Landscape-atmosphere net CH_4 flux	n/a	n/a	0.48	0.58	n/a	0.53
Landscape DOC wet deposition	0.94	1.54	1.00	1.03	1.26	1.15 ± 0.25
Lateral fluxes						
Landscape-stream DOC export	2.94	4.20	3.19	2.91	5.45	3.74 ± 1.09
Landscape-stream DIC export	0.58	0.50	0.59	0.51	0.74	0.58 ± 0.10
Landscape-stream dissolved CO_2 export	0.26	0.26	0.29	0.25	0.43	0.30 ± 0.08
Landscape-stream dissolved CH_4 export	0.0014	0.0012	0.0012	0.0009	0.0012	0.0012 ± 0.0002
Harvest C export	40	8	11	30	27	23 ± 13
NLCB	127	36	146	180	149	128 ± 55

* *Unit in g C m^{-2} yr^{-1}. Landscape-scale GPP, RE, and net CO_2 and CH_4 fluxes follow the micrometeorological sign convention that positive and negative values represent carbon release from and uptake by the landscape, respectively, whereas the opposite ecological sign convention applies to NLCB.*

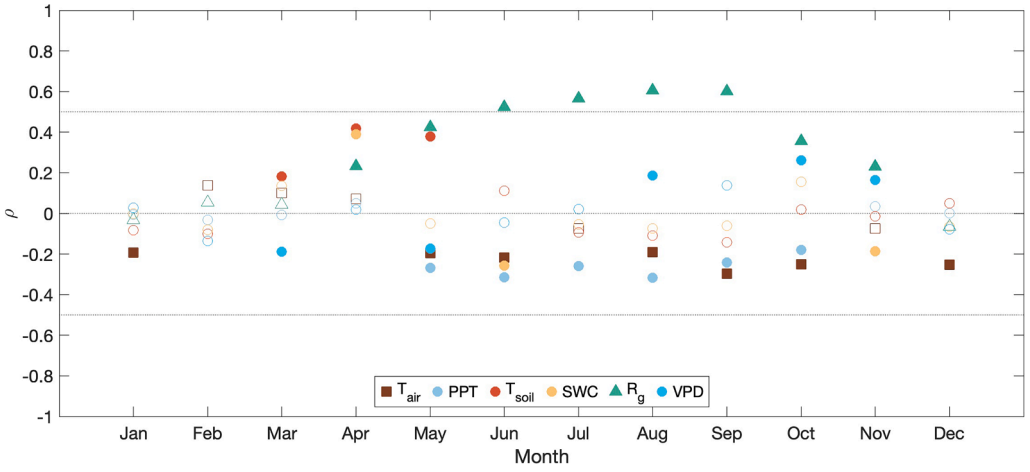

Fig. 4. Partial correlation coefficients (ρ) between daily $NLCB_e$ and environmental factors in each month during the study period of 2016–2020. Environmental factors include air temperature (T_{air}), precipitation (PPT), soil temperature (T_{soil}), soil water content (SWC), global radiation (R_g), and vapor pressure deficit (VPD). Filled markers represent significant correlations ($p < 0.05$).

positively correlated with $NLCB_e$ in the subsequent month, particularly pronounced in June 2018 when the increased $NLCB_e$ followed the elevated T_{air} in May 2018 (Figs. 2a, S9). Dryness also created additional $NLCB_e$ responses during the warm GS in 2018 and 2019. However, we observed contrasting responses of $NLCB_e$ during the early and late drought summer periods. Specifically, $NLCB_e$ and its components were enhanced when the warm and dry conditions occurred during the early stage of GS (May 2018) or when such conditions were moderate in June 2018 (Fig. 2). However, when the warm and dry conditions became severe with both high VPD (up to 15 hPa) and low SWC (15–20 %), terrestrial carbon fluxes including GPP and CH_4 were inhibited in July 2018 and in August 2019 with the largest reduction in GPP by 21 g C m^{-2} in July 2018 (Figs. 2, S9). DOC, DIC, and dissolved CO_2 and CH_4 exports through stream discharge were also reduced in these two months by one-third of their 5-year averages (Fig. 2g-j). The increased DOC deposition via precipitation by 0.08 g C m^{-2} $month^{-1}$ (50 %) was attributed to the occasional thunderstorms that occurred after the drought events but within the same months (Figs. 2f, S10). Altogether, these contrasting drought responses were counterbalanced, resulting in a GS-cumulative $NLCB_e$ in 2018 that was comparable to that of the 5-year mean (266 vs. 252 g C m^{-2}).

The warm GS of 2020 also resulted in a considerable carbon sink with a cumulative $NLCB_e$ of 264 g C m^{-2} over April-October. Different responses in $NLCB_e$ were found between 2017 and 2020 when wet conditions occurred during both NGS periods. Specifically, an increased landscape carbon source magnitude by 42 g C m^{-2} (47 %) was observed during the NGS 2017 mainly through increasing RE by 36 g C m^{-2} (36 %). In contrast, the extremely warm and wet NGS 2020 did not affect the terrestrial carbon fluxes much (mainly RE during NGS) but resulted in an increased amount of carbon losses through stream discharge by 1.3 g C m^{-2} (232 %) compared to the 5-year mean (Fig. 2g-j). The extremely warm and wet conditions even extended the CO_2 uptake (GPP = −12 g C m^{-2} $month^{-1}$) throughout November 2020 (Fig. 2c).

3.4. Impacts of landscape heterogeneity on the $NLCB_e$-responses to environmental factors

Analysis of the spatial heterogeneity in the land cover types and forest aboveground biomass across the landscape showed that mires are dominantly located north of the flux tower and forests with higher aboveground biomass are distributed south of the tower in the central Krycklan (Fig. S1). Given the temporal dynamics of forest aboveground biomass contributions ($f_{biomass}$) to the measurement flux footprints (Fig. S11), daily $NLCB_e$ generally increased with the $f_{biomass}$ (Fig. S12). More contributions from large aboveground tree biomass with a footprint-weighted average ($f_{biomass}$) of > 110 Mg ha^{-1} or fewer contributions from mires (f_{mire} < 14 %) corresponded to a net landscape carbon sink (Fig. S12).

Daily $NLCB_e$ generally increased with increasing T_{air}, T_{soil}, and R_g, but decreased with increasing PPT and SWC. The Belsley collinearity diagnostics suggested that these environmental factors did not exhibit multicollinearity at the daily scale (Table S3). The sensitivities of $NLCB_e$ to all these environmental factors were amplified at a higher $f_{biomass}$ range (>100 Mg ha^{-1}) (Fig. 5). Depending on $f_{biomass}$ or f_{mire}, we found varying responses of $NLCB_e$ to environmental factors (Figs. 5, S13). The $f_{biomass}$ impact on regulating the $NLCB_e$ response to T_{air} became pronounced when T_{air} was above zero where $f_{biomass}$ showed a positive relationship with $NLCB_e$ for mild (0–10 °C) conditions and a negative relationship for warm (>10 °C) conditions (Fig. 5a). A similar but less pronounced pattern was found for T_{soil} (Fig. 5b). In addition, $f_{biomass}$ had a negative impact on the $NLCB_e$-R_g responses (Fig. 5c) because of the larger RE in dark conditions when R_g was within 0–80 W m^{-2} and the lower CO_2 uptake (smaller GPP magnitude) in a high R_g range (250–300 W m^{-2}) at the higher $f_{biomass}$ range, respectively (Fig. S14a-b). A positive and negative relationship between $NLCB_e$ and $f_{biomass}$ was observed under the low rainfall and dry soil and the high rainfall/wet soil conditions, respectively, with a stronger influence of $f_{biomass}$ under dry conditions (Fig. 5d-e). Consistent responses of $NLCB_e$ to VPD occurred when $f_{biomass}$ ranged above 80 Mg ha^{-1} in such that $NLCB_e$ first increased with VPD and then decreased when VPD exceeded 10 hPa. The $NLCB_e$ peak value shifted towards a lower VPD threshold with increasing $f_{biomass}$ (Fig. 5f). A similar VPD-response pattern was found for GPP, with the GPP inhibition by VPD being more pronounced for higher $f_{biomass}$ (Fig. S14c-d).

4. Discussion

4.1. The actively managed boreal forest landscape is a persistent carbon sink

Our study demonstrates that the managed boreal forest landscape is a persistent carbon sink over the five study years. The carbon sink strength of the studied boreal landscape is around three times higher than the mean of boreal forests (38.5 ± 4.4 g C m^{-2} yr^{-1}) as estimated by Pan et al. (2024). This large difference between the carbon sink of our boreal forest landscape and the boreal mean sink could be primarily attributed to the active forest management in boreal Sweden (Cintas et al., 2017; Högberg et al., 2021; Kauppi et al., 2022). For instance, the peak of the

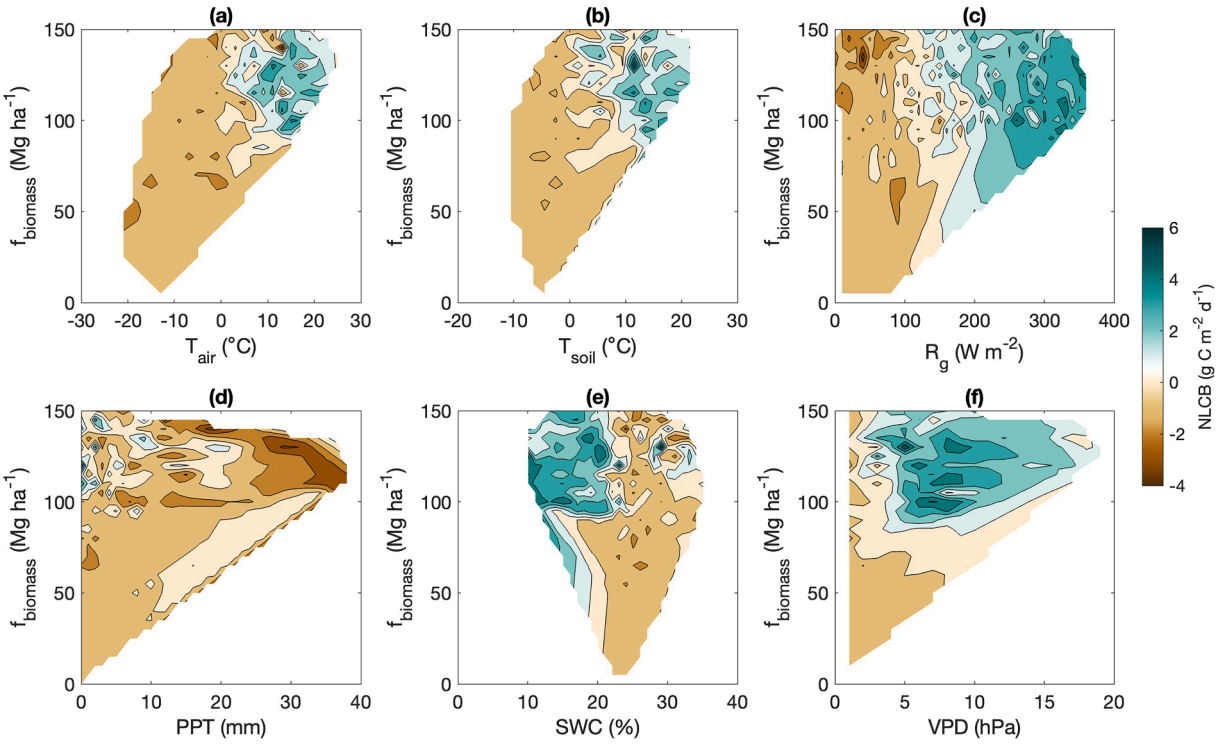

Fig. 5. Responses of daily $NLCB_e$ to environmental factors and forest aboveground biomass contribution ($f_{biomass}$). Environmental factors include daily means of air temperature (T_{air}), precipitation (PPT), soil temperature (T_{soil}), soil water content (SWC), global radiation (R_g), and vapor pressure deficit (VPD). Forest aboveground biomass contribution ($f_{biomass}$) is the sum of the forest AGB estimates across all grid cells within the 90 % footprint contour line weighted by their corresponding source area contributions.

carbon sink (174 ± 62 g C m^{-2} yr^{-1}) occurring in the middle-aged stands and a sustained carbon sink (98 ± 50 g C m^{-2} yr^{-1}) noted in the 131–211 year-old stands located in our studied landscape (Peichl et al., 2023) are both greater than the boreal mean. In comparison, the Canadian managed forests even act as a small carbon source in the 2010s due to the increased impacts of fire and insect disturbances, warming, and droughts (Kurz et al., 2013).

Despite the large inter-annual variations in weather conditions ranging from normal to extremely warm or even wet years, the IAV of the NLCB is relatively limited, featuring only a largely reduced carbon sink during the cool and cloudy year 2017, while the landscape acts as a persistent and considerable carbon sink throughout the other four years. The 5-year study further illustrates that the IAV of the NLCB corresponds most closely with the IAV of annual RE, regardless of the flux partitioning approaches used (Fig. S15). The dominance of RE variations in regulating the temporal variations of NLCB in our study may be caused by the correlation between RE and the amount of litterfall occurring in the preceding years (Fig. S16). This suggests that the availability of substrates (e.g., litterfall and soil organic compounds) rather than abiotic controls plays a vital role in influencing the IAV of boreal forest carbon balance. However, this RE-dominance in regulating the IAV of NLCB is in contrast with previous ecosystem-level studies of boreal forest sites, which suggests that the variation of GPP in response to springtime weather conditions is the major driver of the inter-annual variations of the net ecosystem carbon balance of boreal forests (e.g., Ahmed et al., 2021; Kljun et al., 2007; Park et al., 2018; Pulliainen et al., 2017; Welp et al., 2007). Our findings also diverge from a 2-year study in the same catchment, which attributes the between-year variations in NLCB to GPP in response to warm spring or cloudy autumn conditions (Chi et al., 2019, 2020). By extending the time series to five years, our study now reveals that RE may be the more important component in regulating the NLCB IAV. Overall, this suggests that while environmental effects on GPP might explain short-term (e.g., between-year) variations, the slower processes related to decomposition might be the main control of the IAV in the NLCB of boreal forest landscapes.

The small net CH_4 source function of our boreal landscape is in contrast to the CH_4 sink commonly observed in upland boreal forests (−1 to −0.2 mg CH_4 m^{-2} d^{-1}) (Kuhn et al., 2021). However, the source function is likely due to the contribution of the interspersed mire areas, which emit CH_4 in the range of 20–80 mg CH_4 m^{-2} d^{-1} (Rinne et al., 2020). This offsetting role of boreal forest sink and mire source functions highlights the importance of land cover type contributions in determining the landscape-scale CH_4 fluxes. When considering that the global warming potential of CH_4 is 84 times stronger relative to CO_2 over a 20-year timescale (IPCC, 2013), the observed landscape-scale CH_4 emissions (60 g CO_2-eq m^{-2} yr^{-1}) counterbalance the net radiative cooling effect of the net CO_2 uptake (−568 g CO_2-eq m^{-2} yr^{-1}) by 11 % in our study. Thus, while the contribution of the CH_4 flux to the NLCB and its IAV are negligible, it is important to account for this non-CO_2 flux in assessments of the forest climate impact.

The correspondence of the IAV of the carbon export via clear-cutting with that of the terrestrial net carbon uptake is likely a coincidence since forest operations are mostly planned years in advance and thus independent of inter-annual variations in the landscape CO_2 uptake. However, the reduced harvest export in 2017 largely contributes to maintaining the persistent landscape carbon sink function even during the year with low terrestrial net carbon uptake. The 5-year mean annual clear-cutting rate (0.8 %) is close to the long-term mean of 1 % for this catchment area with a mean rotation length of 90 years, as reported in the historical records. Such rotation forestry is predominantly applied in the Fennoscandia part of the boreal forest biome (Felton et al., 2020; Laudon et al., 2021a). Taking additional biomass export via thinning and other disturbance-related harvest into consideration, which account for 20 % and 10 % of the total harvest respectively in Sweden (Nilsson et al., 2025), the 5-year mean annual C export via harvest would increase to 33 g C m^{-2} yr^{-1}. Overall, our findings highlight that the

terrestrial landscape carbon uptake exceeds that of the export via harvest, thus leading to continuous carbon accumulation in the managed boreal forest landscape.

4.2. Resilience of the landscape-scale carbon sink to extreme weather events

Two extreme-weather conditions during the study period, i.e., the drought summer of 2018 and the warm and wet winter of 2020, do not significantly alter the landscape-scale carbon sink strength compared to the normal year (2016). In fact, these conditions result in an eight and nine times stronger net carbon uptake, respectively, than during the wet year 2017 when GPP is inhibited by the cool and cloudy autumn (Chi et al., 2020). This resilience contrasts with a plot-level study which reported a 57 % reduction in net ecosystem production (NEP) across 50 diverse forest stands within the same landscape during the 2018 drought year (Martínez-García et al., 2024). It also differs from ecosystem-level EC studies in other boreal forests (Kljun et al., 2007; Lindroth et al., 2020; Welp et al., 2007) and mires (Rinne et al., 2020), which suggest a significant reduction of NEP during drought years. This discrepancy between 'top-down' (tall-tower EC method) and 'bottom-up' (plot- and ecosystem-level upscaling) in estimating the landscape-scale carbon balance is primarily due to a divergence in RE, given that our tall-tower EC data and the forest plot-level estimates by Martínez-García et al. (2024) suggest similar GPP but decreased and increased RE, respectively. This difference is possibly attributed to inhibited respiration from the non-forest ecosystems (e.g., mire, grassland, lake) during the drought event (Fig. S17), which might have counterbalanced the elevated respiration from the forest areas, thus resulting in a limited drought response of RE at the landscape scale.

The daily $NLCB_e$ responses to T_{air} and SWC at different f_{mire} ranges further support a stronger landscape carbon sink strength under warm and dry conditions when mires contribute more to the $NLCB_e$ signals (Fig. S13). However, this observation is contrary to the carbon sink-to-source switch observed in the nearby Degerö mire in 2018 (Rinne et al., 2020). Possibly, mires within the Krycklan catchment might have received steady lateral water inflow from the surrounding high-elevation areas even during the drought event. Local hydrological features related to topography also explain a stable or enhanced carbon sink of other northern Fennoscandia mires during drought (Rinne et al., 2020). This indicates that local landscape characteristics might strongly regulate the response of the landscape carbon balance to drought.

The extremely warm and wet NGS during 2020 results in an early onset and enhanced rates of GPP, elevated RE, and the highest aquatic carbon exports. Besides the warm condition, the enhanced stream flow might have expedited the horizontal nutrient exchanges and hence has fostered the elevated respiration rates during the 2020 NGS. Similar freezing-thawing cycle induced respiration responses are also supported by previous studies conducted in the Tibetan alpine grassland (Wang et al., 2014) and boreal evergreen needle-leaf forests (Gharun et al., 2025). Consequently, the increases in both terrestrial and aquatic carbon fluxes during the warm and wet NGS of 2020 have no significant effect on the annual NLCB. Distinct from the ecosystem-scale EC studies reporting significant impacts of the warm and wet winter on carbon balance (Gharun et al., 2025), our findings therefore imply that the NLCB integrated across the tightly coupled land cover types within the boreal landscape shows a more resilient response to the large IAV of environmental conditions with RE being the dominant regulating component in NLCB.

4.3. $NLCB_e$ response to environmental conditions is modulated by forest biomass and mire area contribution

Our analysis further reveals that forest stands with higher aboveground biomass have amplified carbon flux variations to the environmental conditions compared to the less dense or younger stands with lower aboveground biomass. This might be because those forest stands with higher biomass commonly have the highest net primary production rates (Peichl et al., 2023) and thus a larger potential for variations in response to environmental conditions. Similarly, our light-response analysis shows a non-linear function with the largest CO_2 uptake at given light level in the intermediate biomass class, which aligns with the common patterns in the development of carbon fluxes along age or biomass gradients in managed boreal forests (Coursolle et al., 2012; Goulden et al., 2011; Islam et al., 2024; Peichl et al., 2023). Furthermore, the non-forest ecosystems within the landscape may respond differently to environmental factors than forests. Altogether, this suggests complex landscape-scale carbon cycle-climate interactions in response to forest structure and composition of land cover types.

It is further noteworthy that VPD inhibition on GPP is predominantly shown for the specific $f_{biomass}$ range of >80 Mg ha^{-1} (Fig. 5f), within which the increasing inhibition threshold with decreasing $f_{biomass}$ suggests higher tolerance to atmospheric dryness of forest stands with lower biomass in the boreal region (Mirabel et al., 2023). This may explain that the recently observed decline in boreal forest tree growth due to VPD stress (Laudon et al., 2024; Mirabel et al., 2023) is not apparent at the landscape scale covering forest stands with different age and biomass classes (e.g., $f_{biomass} < 80$ Mg ha^{-1}). Furthermore, the reduction in NPP via declining tree growth might be largely counterbalanced by a concurrent decrease in belowground substrate supply and thus a larger reduction in heterotrophic respiration rates. These non-uniform responses of $NLCB_e$ to various environmental conditions under different forest aboveground biomass levels highlight that landscape heterogeneity in response to forest management may strongly modulate carbon cycle-climate feedback across the boreal region.

4.4. Forest management effects on landscape carbon cycle-climate interactions

Our findings from the footprint analysis suggest that forest management might strongly modulate the response of the forest landscape carbon balance to climatic changes. For instance, prolonging the rotation period, introducing alternative strategies toward continuous cover forest management or enhanced set-aside measures will alter the biomass stock, age structure, surface roughness, and albedo of the boreal landscape. Our results suggest that increases in biomass and age would shift the $NLCB_e$ responses to the key environmental factors (i.e., global radiation, air and soil temperatures, and atmospheric and soil dryness) towards stronger variations and lower tolerance to extreme weather events. However, the altered albedo and surface roughness by forest management may introduce additional biophysical effects of boreal forest landscapes on the climate system. For example, the increased albedo by clear-cutting shows a climate cooling effect (Kalliokoski et al., 2020). Thus, a holistic understanding of the consequences of forest management decisions on the land-atmosphere interactions is critical for developing forest strategies that effectively mitigate climate change.

Numerous studies have explored how the boreal forest carbon balance is affected by management effects such as nitrogen fertilization (Marshall et al., 2023; Tian et al., 2021; Zhao et al., 2022), thinning (Aslan et al., 2024; Lindroth et al., 2018), or drainage (Tong et al., 2022a, 2022b, 2024). However, these studies are commonly carried out at the ecosystem level and it remains unclear how their various effects integrate to a net response of the carbon balance at the landscape scale. While linearity is commonly assumed in bottom-up scaling approaches (Kim et al., 2006; Tang et al., 2013), effects might be non-linear or partly counterbalancing. In particular, impacts of management activities that reach beyond the ecosystem scale, e.g., drainage networks and altered aquatic connectivity, are difficult to quantify in ecosystem-level studies. This highlights the need for landscape-scale assessment of the boreal forest carbon balance to understand the integrated effects of various forest management activities. Tall-tower EC measurements combined with stream monitoring networks and supported by detailed land cover

information from satellite imagery and LiDAR products offer the opportunity to provide such urgently needed landscape-scale assessment and are also critical to validate bottom-up modeling estimates of boreal forest carbon cycle-climate interactions.

5. Conclusions

Our study investigates the temporal variations in the NLCB combined with an extended tall-tower footprint analysis over a five-year study period (2016–2020). The results reveal a persistent annual net carbon sink despite significant inter-annual variability in environmental conditions. Our results further suggest that the inter-annual variations of the NLCB are predominantly driven by the variations in landscape respiration, followed by harvest carbon export variations. In comparison, the contributions of landscape methane emissions and aquatic carbon flux variations to the inter-annual variations of the NLCB are small. Moreover, we observe contrasting responses of the NLCB to environmental factors as a function of aboveground biomass and mire area contributions, which illustrates the important impact of spatial heterogeneity inherent in managed forest landscapes on the NLCB. Overall, our findings underscore the significance of actively managed boreal forests as sustained carbon sinks in the present climatic conditions. Further studies on exploring the effects of the altered harvest intensity and life cycle analysis for the harvested wood products are needed to evaluate the carbon balance and climate impact of the forest sector. As climate change is predicted to further intensify in the boreal region, it is imperative to continue monitoring the carbon exchanges across the biosphere-atmosphere-hydrosphere within the heterogeneous landscapes to enhance our understanding of potential climate-induced tipping points in their carbon dynamics and to inform sustainable forest management strategies that support long-term carbon sequestration goals.

CRediT authorship contribution statement

Jinshu Chi: Writing – original draft, Visualization, Software, Methodology, Investigation, Formal analysis, Data curation, Conceptualization. **Anne Klosterhalfen:** Writing – review & editing, Methodology, Investigation, Data curation. **Mats B. Nilsson:** Writing – review & editing, Methodology, Investigation, Data curation. **Hjalmar Laudon:** Writing – review & editing, Methodology, Investigation, Data curation. **Jörgen Wallerman:** Writing – review & editing, Software, Methodology, Data curation. **Johannes Larson:** Writing – review & editing, Software, Methodology, Data curation. **Anders Lindroth:** Writing – review & editing, Data curation. **Natascha Kljun:** Writing – review & editing, Methodology. **Johan E.S. Fransson:** Writing – review & editing, Methodology. **Tomas Lundmark:** Writing – review & editing, Resources. **Matthias Peichl:** Writing – review & editing, Resources, Project administration, Methodology, Investigation, Funding acquisition, Data curation, Conceptualization.

Declaration of competing interest

The authors declare that they have no known competing financial interests or personal relationships that could have appeared to influence the work reported in this paper.

Acknowledgments

The study was funded by the Swedish Research Council for Environment, Agricultural Sciences and Spatial Planning (FORMAS, grant number 942–2015–49, 2020–01446). Additional financial support from the Kempe Foundations (grants SMK-1743 and JCK-1815) and the Knut and Alice Wallenberg Foundation (grants 2015.0047 and 2018.0259) are also acknowledged. The study site Svartberget contributes to the Swedish Infrastructure for Ecosystem Science (SITES) and the Swedish Integrated Carbon Observation System (ICOS-Sweden) research infrastructure. Financial support from the Swedish Research Council and contributing research institutes to both SITES and ICOS-Sweden are acknowledged. The lead author J.C. gratefully acknowledges the financial support from the Research Grants Council of the Hong Kong Special Administrative Region, China (Project Reference Number: AoE/P-601/23-N), the Guangdong provincial project (2023QN10L516), and the Center for Ocean Research in Hong Kong and Macau (CORE). CORE is a joint research center for ocean research between Laoshan Laboratory and HKUST. N.K. is supported by the Strategic Research Area "Biodiversity and Ecosystem Services in a Changing Climate", BECC, funded by the Swedish government. We thank the staff at the Unit for Field-based Forest Research, SLU, for support in field data collection.

Supplementary materials

Supplementary material associated with this article can be found, in the online version, at doi:10.1016/j.agrformet.2025.110758.

Data availability

The data that support the findings of this study are available in the Zenodo repository at [10.5281/zenodo.14997575].

References

Ahmed, H.F., Helgason, W., Barr, A., Black, A., 2021. Characterization of spring thaw and its relationship with carbon uptake for different types of southern boreal forest. Agric. Meteorol. 307, 108511. https://doi.org/10.1016/j.agrformet.2021.108511.

Aslan, T., Launiainen, S., Kolari, P., Peltola, O., Aalto, J., Bäck, J., Vesala, T., Mammarella, I., 2024. Thinning turned boreal forest to a temporary carbon source - short term effects of partial harvest on carbon dioxide and water vapor fluxes. Agric. Meteorol. 353, 110061. https://doi.org/10.1016/j.agrformet.2024.110061.

Balathandayuthabani, S., Wallin, M.B., Klemedtsson, L., Crill, P., Bastviken, D., 2023. Aquatic carbon fluxes in a hemiboreal catchment are predictable from landscape morphology, temperature, and runoff. Limnol. Oceanogr. Lett. 8 (2), 313–322. https://doi.org/10.1002/lol2.10312.

Bell, B., Hersbach, H., Simmons, A., Berrisford, P., Dahlgren, P., Horányi, A., Muñoz-Sabater, J., Nicolas, J., Radu, R., Schepers, D., Soci, C., Villaume, S., Bidlot, J.R., Haimberger, L., Woollen, J., Buontempo, C., Thépaut, J.N., 2021. The ERA5 global reanalysis: preliminary extension to 1950. Q. J. R. Meteorol. Soc. 147 (741), 4186–4227. https://doi.org/10.1002/qj.4174.

Casas-Ruiz, J.P., Bodmer, P., Bona, K.A., Butman, D., Couturier, M., Emilson, E.J.S., Finlay, K., Genet, H., Hayes, D., Karlsson, J., Paré, D., Peng, C., Striegl, R., Webb, J., Wei, X., Ziegler, S.E., del Giorgio, P.A., 2023. Integrating terrestrial and aquatic ecosystems to constrain estimates of land-atmosphere carbon exchange. Nat. Commun. 14 (1), 1571. https://doi.org/10.1038/s41467-023-37232-2.

Chapin, F.S., Woodwell, G.M., Randerson, J.T., Rastetter, E.B., Lovett, G.M., Baldocchi, D.D., Clark, D.A., Harmon, M.E., Schimel, D.S., Valentini, R., Wirth, C., Aber, J.D., Cole, J.J., Goulden, M.L., Harden, J.W., Heimann, M., Howarth, R.W., Matson, P.A., McGuire, A.D., Melillo, J.M., Mooney, H.A., Neff, J.C., Houghton, R.A., Pace, M.L., Ryan, M.G., Running, S.W., Sala, O.E., Schlesinger, W.H., Schulze, E.D., 2006. Reconciling carbon-cycle concepts, terminology, and methods. Ecosystems 9 (7), 1041–1050. https://doi.org/10.1007/s10021-005-0105-7.

Chasmer, L., Kljun, N., Hopkinson, C., Brown, S., Milne, T., Giroux, K., Barr, A.G., Devito, K., Petrone, R., 2011. Characterizing vegetation structural and topographic characteristics sampled by eddy covariance within two mature Aspen stands using LiDAR and a Flux Footprint Model: scaling to MODIS. J. Geophys. Res. Biogeosci. 116, G02026. https://doi.org/10.1029/2010JG001567.

Chi, J., Nilsson, M.B., Kljun, N., Wallerman, J., Fransson, J.E.S., Laudon, H., Lundmark, T., Peichl, M., 2019. The carbon balance of a managed boreal landscape measured from a tall tower in northern Sweden. Agric. Meteorol. 274, 29–41. https://doi.org/10.1016/j.agrformet.2019.04.010.

Chi, J., Nilsson, M.B., Laudon, H., Lindroth, A., Wallerman, J., Fransson, J.E.S., Kljun, N., Lundmark, T., Ottosson Löfvenius, M., Peichl, M., 2020. The Net landscape carbon balance—Integrating terrestrial and aquatic carbon fluxes in a managed boreal forest landscape in Sweden. Glob. Chang. Biol. 26 (4), 2353–2367. https://doi.org/10.1111/gcb.14983.

Christensen, T.R., Johansson, T., Olsrud, M., Strom, L., Lindroth, A., Mastepanov, M., Malmer, N., Friborg, T., Crill, P., Callaghan, T.V., 2007. A catchment-scale carbon and greenhouse gas budget of a subarctic landscape. Philos. Trans. R. Soc. A 365 (1856), 1643–1656. https://doi.org/10.1098/rsta.2007.2035.

Cintas, O., Berndes, G., Hansson, J., Poudel, B.C., Bergh, J., Börjesson, P., Egnell, G., Lundmark, T., Nordin, A., 2017. The potential role of forest management in Swedish scenarios towards climate neutrality by mid century. For. Ecol. Manage 383, 73–84. https://doi.org/10.1016/j.foreco.2016.07.015.

Coursolle, C., Margolis, H.A., Giasson, M.A., Bernier, P.Y., Amiro, B.D., Arain, M.A., Barr, A.G., Black, T.A., Goulden, M.L., McCaughey, J.H., Chen, J.M., Dunn, A.L.,

Grant, R.F., Lafleur, P.M., 2012. Influence of stand age on the magnitude and seasonality of carbon fluxes in Canadian forests. Agric. Meteorol. 165, 136–148. https://doi.org/10.1016/j.agrformet.2012.06.011.

Drysdale, W.S., Vaughan, A.R., Squires, F.A., Cliff, S.J., Metzger, S., Durden, D., Pingintha-Durden, N., Helfter, C., Nemitz, E., Grimmond, C.S.B., Barlow, J., Beevers, S., Stewart, G., Dajnak, D., Purvis, R.M., Lee, J.D., 2022. Eddy covariance measurements highlight sources of nitrogen oxide emissions missing from inventories for central London. Atmos. Chem. Phys. 22 (14), 9413–9433. https://doi.org/10.5194/acp-22-9413-2022.

Duvert, C., Hutley, L.B., Beringer, J., Bird, M.I., Birkel, C., Maher, D.T., Northwood, M., Rudge, M., Setterfield, S.A., Wynn, J.G., 2020. Net landscape carbon balance of a tropical savanna: relative importance of fire and aquatic export in offsetting terrestrial production. Glob. Chang. Biol. 26 (10), 5899–5913. https://doi.org/10.1111/gcb.15287.

Felton, A., Löfroth, T., Angelstam, P., Gustafsson, L., Hjältén, J., Felton, A.M., Simonsson, P., Dahlberg, A., Lindbladh, M., Svensson, J., Nilsson, U., Lodin, I., Hedwall, P.O., Sténs, A., Lämås, T., Brunet, J., Kalén, C., Kriström, B., Gemmel, P., Ranius, T., 2020. Keeping pace with forestry: multi-scale conservation in a changing production forest matrix. Ambio 49 (5), 1050–1064. https://doi.org/10.1007/s13280-019-01248-0.

Gao, Y., Jia, J., Lu, Y., Sun, K., Wang, J., Wang, S., 2022. Carbon transportation, transformation, and sedimentation processes at the land-river-estuary continuum. Fundam. Res. https://doi.org/10.1016/j.fmre.2022.07.007.

Gauthier, S., Bernier, P., Kuuluvainen, T., Shvidenko, A.Z., Schepaschenko, D.G., 2015. Boreal forest health and global change. Science 349 (6250), 819–822. https://doi.org/10.1126/science.aaa9092.

Gharun, M., Shekhar, A., Hörtnagl, L., Krebs, L., Arriga, N., Migliavacca, M., Roland, M., Gielen, B., Montagnani, L., Tomelleri, E., Šigut, L., Peichl, M., Zhao, P., Schmidt, M., Grünwald, T., Korkiakoski, M., Lohila, A., Buchmann, N., 2025. Impact of winter warming on CO_2 fluxes in evergreen needleleaf forests. Biogeosciences 22, 1393–1411. https://doi.org/10.5194/bg-22-1393-2025.

Gómez-Gener, L., Lupon, A., Laudon, H., Sponseller, R.A., 2020. Drought alters the biogeochemistry of boreal stream networks. Nat. Commun. 11 (1), 1795. https://doi.org/10.1038/s41467-020-15496-2.

Goulden, M.L., McMillan, A.M.S., Winston, G.C., Rocha, A.V., Manies, K.L., Harden, J.W., Bond-Lamberty, B.P., 2011. Patterns of NPP, GPP, respiration, and NEP during boreal forest succession. Glob. Chang. Biol. 17 (2), 855–871. https://doi.org/10.1111/j.1365-2486.2010.02274.x.

Goulden, M.L., Munger, J.W., Fan, S.M., Daube, B.C., Wofsy, S.C., 1996. Measurements of carbon sequestration by long-term eddy covariance: methods and a critical evaluation of accuracy. Glob. Chang. Biol. 2 (3), 169–182. https://doi.org/10.1111/j.1365-2486.1996.tb00070.x.

Heiskanen, L., Tuovinen, J.P., Vekuri, H., Räsänen, A., Virtanen, T., Juutinen, S., Lohila, A., Mikola, J., Aurela, M., 2023. Meteorological responses of carbon dioxide and methane fluxes in the terrestrial and aquatic ecosystems of a subarctic landscape. Biogeosciences 20 (3), 545–572. https://doi.org/10.5194/bg-20-545-2023.

Helbig, M., Chasmer, L.E., Kljun, N., Quinton, W.L., Treat, C.C., Sonnentag, O., 2017. The positive net radiative greenhouse gas forcing of increasing methane emissions from a thawing boreal forest-wetland landscape. Glob. Chang. Biol. 23 (6), 2413–2427. https://doi.org/10.1111/gcb.13520.

Högberg, P., Ceder, L.A., Astrup, R., Binkley, D., Bright, R., Dalsgaard, L., Egnell, G., Filipchuk, A., Genet, H., Ilintsev, A., Kurz, W.A., Laganière, J., Lemprière, Y., Lundblad, M., Lundmark, T., Mäkipää, R., Malysheva, N., Mohr, C.W., Nordin, A., Petersson, H., Repo, A., Schepaschenko, D., Shvidenko, A., Soegaard, G., Kraxneret, F., 2021. Report from an Insight Process conducted by a team appointed by the International Boreal Forest Research Association (IBFRA). Swedish Forest Agency Report No. 11.

IPCC, 2013. Climate change 2013: the physical science basis. Contribution of Working Group I to the Fifth Assessment Report of the Intergovernmental Panel On Climate Change. Cambridge University Press, Cambridge, United Kingdom and New York, NY, USA.

IPCC, 2023. In: Lee, H., Romero, J. (Eds.), Climate Change 2023: Synthesis Report. Contribution of Working Groups I, II and III to the Sixth Assessment Report of the Intergovernmental Panel On Climate Change [Core Writing Team. IPCC, Geneva, Switzerland.

Islam, Md.R., Jönsson, A.M., Bergkvist, J., Lagergren, F., Lindeskog, M., Mölder, M., Scholze, M., Kljun, N., 2024. Projected effects of climate change and forest management on carbon fluxes and biomass of a boreal forest. Agric. Meteorol. 349, 109959. https://doi.org/10.1016/j.agrformet.2024.109959.

Kalliokoski, T., Bäck, J., Boy, M., Kulmala, M., Kuusinen, N., Mäkelä, A., Minkkinen, K., Minunno, F., Paasonen, P., Teltoniemi, M., Taipale, D., Valsta, L., Vanhatalo, A., Zhou, L., Zhou, P., Berninger, F., 2020. Mitigation impact of different harvest scenarios of Finnish forests that account for albedo, aerosols, and trade-offs of carbon sequestration and avoided emissions. Front. For. Glob. Change 3, 562044. https://doi.org/10.3389/ffgc.2020.562044.

Kauppi, P.E., Stål, G., Arnesson-Ceder, L., Hallberg Sramek, I., Hoen, H.F., Svensson, A., Wernick, I.K., Högberg, P., Lundmark, T., Nordin, A., 2022. Managing existing forests can mitigate climate change. For. Ecol. Manage 513, 120186. https://doi.org/10.1016/j.foreco.2022.120186.

Kim, J., Guo, Q., Baldocchi, D.D., Leclerc, M.Y., Xu, L., Schmid, H.P., 2006. Upscaling fluxes from tower to landscape: overlaying flux footprints on high-resolution (IKONOS) images of vegetation cover. Agric. Meteorol. 136 (3–4), 132–146. https://doi.org/10.1016/j.agrformet.2004.11.015.

Kljun, N., Black, T.A., Griffis, T.J., Barr, A.G., Gaumont-Guay, D., Morgenstern, K., McCaughey, J.H., Nesic, Z., 2007. Response of net ecosystem productivity of three boreal forest stands to drought. Ecosystems 10, 1039–1055. https://doi.org/10.1007/s10021-007-9088-x.

Kljun, N., Calanca, P., Rotach, M.W., Schmid, H.P., 2015. A simple two-dimensional parameterisation for flux footprint prediction (FFP). Geosci. Model. Dev. 8 (11), 3695–3713. https://doi.org/10.5194/gmd-8-3695-2015.

Klosterhalfen, A., Chi, J., Kljun, N., Lindroth, A., Laudon, H., Nilsson, M.B., Peichl, M., 2023. Two-level eddy covariance measurements reduce bias in land-atmosphere exchange estimates over a heterogeneous boreal forest landscape. Agric. Meteorol. 339, 109523. https://doi.org/10.1016/j.agrformet.2023.109523.

Kuhn, M.A., Varner, R.K., Bastviken, D., Crill, P., MacIntyre, S., Turetsky, M., Walter Anthony, K., McGuire, A.D., Olefeldt, D., 2021. BAWLD-CH_4: a comprehensive dataset of methane fluxes from boreal and arctic ecosystems. Earth. Syst. Sci. Data 13 (11), 5151–5189. https://doi.org/10.5194/essd-13-5151-2021.

Kurz, W.A., Shaw, C.H., Boisvenue, C., Stinson, G., Metsaranta, J., Leckie, D., Dyk, A., Smyth, C., Neilson, E.T., 2013. Carbon in Canada's boreal forest - A synthesis. Environ. Rev. 21 (4), 260–292. https://doi.org/10.1139/er-2013-0041.

Laudon, H., Berggren, M., Ågren, A., Buffam, I., Bishop, K., Grabs, T., Jansson, M., Kohler, S., 2011. Patterns and dynamics of dissolved organic carbon (DOC) in boreal streams: the role of processes, connectivity, and scaling. Ecosystems 14 (6), 880–893. https://doi.org/10.1007/s10021-011-9452-8.

Laudon, H., Hasselquist, E.M., Peichl, M., Lindgren, K., Sponseller, R., Lidman, F., Kuglerová, L., Hasselquist, N.J., Bishop, K., Nilsson, M.B., Ågren, A.M., 2021a. Northern landscapes in transition: evidence, approach and ways forward using the Krycklan Catchment Study. Hydrol. Process. 35 (4), e14170. https://doi.org/10.1002/hyp.14170.

Laudon, H., Mensah, A.A., Fridman, J., Näsholm, T., Jämtgård, S., 2024. Swedish forest growth decline: a consequence of climate warming? For. Ecol. Manage 565, 122052. https://doi.org/10.1016/j.foreco.2024.122052.

Laudon, H., Sponseller, R.A., Bishop, K., 2021b. From legacy effects of acid deposition in boreal streams to future environmental threats. Environ. Res. Lett. 16 (1), 015007. https://doi.org/10.1088/1748-9326/abd064.

Lindroth, A., Holst, J., Heliasz, M., Vestin, P., Lagergren, F., Biermann, T., Cai, Z., Mölder, M., 2018. Effects of low thinning on carbon dioxide fluxes in a mixed hemiboreal forest. Agric. Meteorol. 262, 59–70. https://doi.org/10.1016/j.agrformet.2018.06.021.

Lindroth, A., Holst, J., Linderson, M., Aurela, M., Biermann, T., Heliasz, M., Chi, J., Ibrom, A., Kolari, P., Klemedtsson, L., Krasnova, A., Laurila, T., Lehner, I., Lohila, A., Mammarella, I., Mölder, M., Ottoson Löfvenius, M., Peichl, M., Pilegaard, K., Soosar, K., Vesala, T., Vestin, P., Weslien, P., Nilsson, M., 2020. Effects of drought and meteorological forcing on carbon and water fluxes in Nordic forests during the dry summer of 2018. Philos. Trans. R. Soc. B 375 (1810), 20190516. https://doi.org/10.1098/rstb.2019.0516.

Liu, B., Wang, Z., Tian, M., Yang, X., Chan, C.N., Chen, S., Yang, Q., Ran, L., 2023. Basin-scale CO_2 emissions from the East river in south China: importance of small rivers, human impacts and monsoons. J. Geophys. Res. 128 (1), e2022JG007291. https://doi.org/10.1029/2022JG007291.

Lv, S., Yu, Q., Wang, L., Deng, C., Liu, L., 2023. Downstream carbon transport and surface CO_2 evasion in the Hanjiang River Network and their implications for regional carbon budget. Sci. Total. Environ. 884, 163839. https://doi.org/10.1016/j.scitotenv.2023.163839.

Marshall, J.D., Tarvainen, L., Zhao, P., Lim, H., Wallin, G., Näsholm, T., Lundmark, T., Linder, S., Peichl, M., 2023. Components explain, but do eddy fluxes constrain? Carbon budget of a nitrogen-fertilized boreal Scots pine forest. New. Phytol. 239 (6), 2166–2179. https://doi.org/10.1111/nph.18939.

Martínez-García, E., Nilsson, M.B., Laudon, H., Lundmark, T., Fransson, J.E.S., Wallerman, J., Peichl, M., 2022. Overstory dynamics regulate the spatial variability in forest-floor CO_2 fluxes across a managed boreal forest landscape. Agric. Meteorol. 318, 108916. https://doi.org/10.1016/j.agrformet.2022.108916.

Martínez-García, E., Nilsson, M.B., Laudon, H., Lundmark, T., Fransson, J.E.S., Wallerman, J., Peichl, M., 2024. Drought response of the boreal forest carbon sink is driven by understorey–tree composition. Nat. Geosci. 17 (3), 197–204. https://doi.org/10.1038/s41561-024-01374-9.

Mauder, M. and Foken, T., 2004. Documentation and instruction manual of the eddy covariance software package TK2. 1–67.

Mirabel, A., Girardin, M.P., Metsaranta, J., Way, D., Reich, P.B., 2023. Increasing atmospheric dryness reduces boreal forest tree growth. Nat. Commun. 14 (1), 6901. https://doi.org/10.1038/s41467-023-42466-1.

Moffat, A.M., Papale, D., Reichstein, M., Hollinger, D.Y., Richardson, A.D., Barr, A.G., Beckstein, C., Braswell, B.H., Churkina, G., Desai, A.R., Falge, E., Gove, J.H., Heimann, M., Hui, D.F., Jarvis, A.J., Kattge, J., Noormets, A., Stauch, V.J., 2007. Comprehensive comparison of gap-filling techniques for eddy covariance net carbon fluxes. Agric. Meteorol. 147 (3–4), 209–232. https://doi.org/10.1016/j.agrformet.2007.08.011.

Montagnani, L., Grünwald, T., Kowalski, A., Mammarella, I., Merbold, L., Metzger, S., Sedlák, P., Siebicke, L., 2018. Estimating the storage term in eddy covariance measurements: the ICOS methodology. Int. Agrophys. 32, 551–567. https://doi.org/10.1515/intag-2017-0037.

Nillson, P., Markström, M., Fridman, J., 2025. Forest statistics 2025. Official Statistics of Sweden. Swedish University of Agricultural Sciences, Umeå.

Pan, Y., Birdsey, R.A., Fang, J., Houghton, R.A., Kauppi, P.E., Kurz, W.A., Phillips, O.L., Shvidenko, A., Lewis, S.L., Canadell, J.G., Ciais, P., Jackson, R.B., Pacala, S.W., McGuire, A.D., Piao, S., Rautiainen, A., Sitch, S., Hayes, D., 2011. A large and persistent carbon sink in the world's forests. Science 333 (6045), 988–993. https://doi.org/10.1126/science.1201609.

Pan, Y., Birdsey, R.A., Phillips, O.L., Houghton, R.A., Fang, J., Kauppi, P.E., Keith, H., Kurz, W.A., Ito, A., Lewis, S.L., Nabuurs, G.J., Shvidenko, A., Hashimoto, S.,

Lerink, B., Schepaschenko, D., Castanho, A., Murdiyarso, D., 2024. The enduring world forest carbon sink. Nature 631 (8021), 563–569. https://doi.org/10.1038/s41586-024-07602-x.

Park, H., Jeong, S.J., Ho, C.H., Park, C.E., Kim, J., 2018. Slowdown of spring green-up advancements in boreal forests. Remote Sens. Env. 217, 191–202. https://doi.org/10.1016/j.rse.2018.08.012.

Peichl, M., Martínez-García, E., Fransson, J.E.S., Wallerman, J., Laudon, H., Lundmark, T., Nilsson, M.B., 2023. Landscape-variability of the carbon balance across managed boreal forests. Glob. Chang. Biol. 29 (4), 1119–1132. https://doi.org/10.1111/gcb.16534.

Pulliainen, J., Aurela, M., Laurila, T., Aalto, T., Takala, M., Salminen, M., Kulmala, M., Barr, A., Heimann, M., Lindroth, A., Laaksonen, A., Derksen, C., Mäkelä, A., Markkanen, T., Lemmetyinen, J., Susiluoto, J., Dengel, S., Mammarella, I., Tuovinen, J.P., Vesala, T., 2017. Early snowmelt significantly enhances boreal springtime carbon uptake. Proc. Natl. Acad. Sci. 114 (42), 11081–11086. https://doi.org/10.1073/pnas.1707889114.

Ran, L., Wang, X., Li, S., Zhou, Y., Xu, Y.J., Chan, C.N., Fang, N., Xin, Z., Shen, H., 2022. Integrating aquatic and terrestrial carbon fluxes to assess the net landscape carbon balance of a highly erodible semiarid catchment. J. Geophys. Res. 127 (3), e2021JG006765. https://doi.org/10.1029/2021JG006765.

Reichstein, M., Falge, E., Baldocchi, D., Papale, D., Aubinet, M., Berbigier, P., Bernhofer, C., Buchmann, N., Gilmanov, T., Granier, A., Grunwald, T., Havrankova, K., Ilvesniemi, H., Janous, D., Knohl, A., Laurila, T., Lohila, A., Loustau, D., Matteucci, G., Meyers, T., Miglietta, F., Ourcival, J.M., Pumpanen, J., Rambal, S., Rotenberg, E., Sanz, M., Tenhunen, J., Seufert, G., Vaccari, F., Vesala, T., Yakir, D., Valentini, R., 2005. On the separation of net ecosystem exchange into assimilation and ecosystem respiration: review and improved algorithm. Glob. Chang. Biol. 11 (9), 1424–1439. https://doi.org/10.1111/j.1365-2486.2005.001002.x.

Rinne, J., Tuovinen, J.P., Klemedtsson, L., Aurela, M., Holst, J., Lohila, A., Weslien, P., Vestin, P., Łakomiec, P., Peichl, M., Tuittila, E.S., Heiskanen, L., Laurila, T., Li, X., Alekseychik, P., Mammarella, I., Ström, L., Crill, P., Nilsson, M.B., 2020. Effect of the 2018 European drought on methane and carbon dioxide exchange of northern mire ecosystems. Philos. Trans. R. Soc. B 375 (1810), 20190517. https://doi.org/10.1098/rstb.2019.0517.

Song, X., Lyu, S., Sun, K., Gao, Y., Wen, X., 2021. Flux and source of dissolved inorganic carbon in a headwater stream in a subtropical plantation catchment. J Hydrol 600, 126511. https://doi.org/10.1016/j.jhydrol.2021.126511.

Tang, R.L., Li, Z.L., Sun, X.M., 2013. Temporal upscaling of instantaneous evapotranspiration: an intercomparison of four methods using eddy covariance measurements and MODIS data. Remote Sens Env. 138, 102–118. https://doi.org/10.1016/j.rse.2013.07.001.

Tian, X., Minunno, F., Schiestl-Aalto, P., Chi, J., Zhao, P., Peichl, M., Marshall, J., Näsholm, T., Lim, H., Peltoniemi, M., Linder, S., Mäkelä, A., 2021. Disaggregating the effects of nitrogen addition on gross primary production in a boreal Scots pine forest. Agric. Meteorol. 301-302, 108337. https://doi.org/10.1016/j.agrformet.2021.108337.

Tong, C.H.M., Nilsson, M.B., Drott, A., Peichl, M., 2022a. Drainage ditch cleaning has no impact on the carbon and greenhouse gas balances in a recent forest clear-cut in boreal Sweden. Forests. 13 (6), 842. https://doi.org/10.3390/f13060842.

Tong, C.H.M., Nilsson, M.B., Sikström, U., Ring, E., Drott, A., Eklöf, K., Futter, M.N., Peacock, M., Segersten, J., Peichl, M., 2022b. Initial effects of post-harvest ditch cleaning on greenhouse gas fluxes in a hemiboreal peatland forest. Geoderma 426, 116055. https://doi.org/10.1016/j.geoderma.2022.116055.

Tong, C.H.M., Noumonvi, K.D., Ratcliffe, J., Laudon, H., Järveoja, J., Drott, A., Nilsson, M.B., Peichl, M., 2024. A drained nutrient-poor peatland forest in boreal Sweden constitutes a net carbon sink after integrating terrestrial and aquatic fluxes. Glob. Chang. Biol. 30 (3), e17246. https://doi.org/10.1111/gcb.17246.

Wallin, M., Buffam, I., Öquist, M., Laudon, H., Bishop, K., 2010. Temporal and spatial variability of dissolved inorganic carbon in a boreal stream network: concentrations and downstream fluxes. J. Geophys. Res. 115, G02014. https://doi.org/10.1029/2009jg001100.

Wallin, M., Grabs, T., Buffam, I., Laudon, H., Ågren, A., Öquist, M.G., Bishop, K., 2013. Evasion of CO_2 from streams - the dominant component of the carbon export through the aquatic conduit in a boreal landscape. Glob. Chang. Biol. 19 (3), 785–797. https://doi.org/10.1111/gcb.12083.

Wang, Y., Liu, H., Chung, H., Yu, L., Mi, Z., Geng, Y., Jing, X., Wang, S., Zeng, H., Cao, G., Zhao, X., He, J.S., 2014. Non-growing-season soil respiration is controlled by freezing and thawing processes in the summer monsoon-dominated Tibetan alpine grassland. Glob. Biogeochem. Cycles 28 (10), 1081–1095. https://doi.org/10.1002/2013GB004760.

Webb, J.R., Santos, I.R., Maher, D.T., Finlay, K., 2019. The importance of aquatic carbon fluxes in net ecosystem carbon budgets: a catchment-scale review. Ecosystems 22 (3), 508–527. https://doi.org/10.1007/s10021-018-0284-7.

Webb, J.R., Santos, I.R., Maher, D.T., Macdonald, B., Robson, B., Isaac, P., McHugh, I., 2018. Terrestrial versus aquatic carbon fluxes in a subtropical agricultural floodplain over an annual cycle. Agric. Meteorol. 260-261, 262–272. https://doi.org/10.1016/j.agrformet.2018.06.015.

Welp, L.R., Randerson, J.T., Liu, H.P., 2007. The sensitivity of carbon fluxes to spring warming and summer drought depends on plant functional type in boreal forest ecosystems. Agric. Meteorol. 147 (3), 172–185. https://doi.org/10.1016/j.agrformet.2007.07.010.

Wharton, S., Schroeder, M., Paw U, K.T., Falk, M., Bible, K., 2009. Turbulence considerations for comparing ecosystem exchange over old-growth and clear-cut stands for limited fetch and complex canopy flow conditions. Agric. Meteorol. 149 (9), 1477–1490. https://doi.org/10.1016/j.agrformet.2009.04.002.

Wutzler, T., Lucas-Moffat, A., Migliavacca, M., Knauer, J., Sickel, K., Šigut, L., Menzer, O., Reichstein, M., 2018. Basic and extensible post-processing of eddy covariance flux data with REddyProc. Biogeosciences 15 (16), 5015–5030. https://doi.org/10.5194/bg-15-5015-2018.

Zhao, J., Chi, J., Jocher, G., 2023. Editorial: greenhouse gas fluxes in forest ecosystems. Front. For. Glob. Change 6. https://doi.org/10.3389/ffgc.2023.1200668.

Zhao, P., Chi, J., Nilsson, M.B., Löfvenius, M.O., Högberg, P., Jocher, G., Lim, H., Mäkelä, A., Marshall, J., Ratcliffe, J., Tian, X., Näsholm, T., Lundmark, T., Linder, S., Peichl, M., 2022. Long-term nitrogen addition raises the annual carbon sink of a boreal forest to a new steady-state. Agric. Meteorol. 324, 109112. https://doi.org/10.1016/j.agrformet.2022.109112.